RESEARCH ARTICLE

Human Mutation

OFFICIAL JOURNAL HGVS HUMAN GENOME VARIATION SOCIETY www.hgvs.org

Large Deletions of the *KCNV2* Gene are Common in Patients with Cone Dystrophy with Supernormal Rod Response

Bernd Wissinger,[1]* Simone Schaich,[1] Britta Baumann,[1] Michael Bonin,[2] Herbert Jägle,[3]† Christoph Friedburg,[4] Balázs Varsányi,[5] Carel B. Hoyng,[6] Hélène Dollfus,[7] John R. Heckenlively,[8] Thomas Rosenberg,[9] Günter Rudolph,[10] Ulrich Kellner,[11] Roberto Salati,[12] Astrid Plomp,[13,14] Elfride De Baere,[15] Monika Andrassi-Darida,[4] Alexandra Sauer,[1] Christiane Wolf,[1] Ditta Zobor,[3] Antje Bernd,[3] Bart P. Leroy,[15,16] Péter Enyedi,[17] Frans P.M. Cremers,[18] Birgit Lorenz,[4] Eberhart Zrenner,[3] and Susanne Kohl[1]

[1]Molecular Genetics Laboratory, Institute for Ophthalmic Research, Centre for Ophthalmology, University Clinics Tübingen, Germany; [2]Department of Medical Genetics, Institute for Human Genetics, University of Tübingen, Germany; [3]University Eye Hospital, Centre for Ophthalmology, University Clinics Tübingen, Germany; [4]Department of Ophthalmology, Justus-Liebig-University Giessen, Giessen, Germany; [5]Department of Ophthalmology, Semmelweis University, Budapest, Hungary; [6]Department of Ophthalmology, Radboud University Nijmegen Medical Centre, Nijmegen, The Netherlands; [7]Centre de Référence pour les Affections Rare en Génétique Ophthalmologique, Hôpitaux Universitaires de Strasbourg, Strasbourg, France; [8]Kellogg Eye Center, University of Michigan, Ann Arbor, MI; [9]Gordon Norrie Centre for Genetic Eye Diseases, National Eye Clinic, Kennedy Center, Hellerup, Denmark; [10]University Eye Hospital, Ludwigs-Maximilians-University, Munich, Germany; [11]Retina Science, Bonn, Germany; [12]IRCCS Eugenio Medea, Bosisio Parini, Italy; [13]Department of Clinical and Molecular Ophthalmogenetics, Netherlands Institute for Neuroscience and Institute of the Royal Netherlands Academy of Arts and Sciences, Amsterdam, The Netherlands; [14]Department of Clinical Genetics, Academic Medical Center, Amsterdam, The Netherlands; [15]Center for Medical Genetics, Ghent University Hospital & Ghent University, Belgium; [16]Department of Ophthalmology, Ghent University Hospital & Ghent University, Belgium; [17]Department of Physiology, Semmelweis University of Medicine, Budapest, Hungary; [18]Department of Human Genetics, Radboud University Nijmegen Medical Centre, The Netherlands

Communicated by Andreas Gal

Received 22 October 2010; accepted revised manuscript 11 July 2011.
Published online 29 August 2011 in Wiley Online Library (www.wiley.com/humanmutation).DOI: 10.1002/humu.21580

ABSTRACT: Cone dystrophy with supernormal rod response (CDSRR) is considered to be a very rare autosomal recessive retinal disorder. CDSRR is associated with mutations in *KCNV2*, a gene that encodes a modulatory subunit (Kv8.2) of a voltage-gated potassium channel. In this study, we found that *KCNV2* mutations are present in a substantial fraction (2.2–4.3%) of a sample of 367 independent patients with a variety of initial clinical diagnoses of cone malfunction, indicating that CDSRR is underdiagnosed and more common than previously thought. In total, we identified 20 different *KCNV2* mutations; 15 of them are novel. A new finding of this study is the substantial proportion of large deletions at the *KCNV2* locus that accounts for 15.5% of the mutant alleles in our sample. We determined the breakpoints and size of all five different deletions, which ranged between 10.9 and 236.8 kb. Two deletions encompass the entire *KCNV2* gene and one also includes the adjacent *VLDLR* gene. Furthermore, we investigated N-terminal amino acid substitution mutations for its effect on interaction with Kv2.1 using yeast two-hybrid technology. We found that these mutations dramatically reduce or abolish this interaction suggesting a lack of assembly of heteromeric Kv channels as one underlying pathomechanism of CDSRR.
Hum Mutat 32:1398–1406, 2011.

KEY WORDS: retinal dystrophy; deletion; Kv channel; *KCNV2*

Introduction

Mutations in the *KCNV2* gene (MIM# 607604) has been recently identified to cause a peculiar form inherited retinopathy known as cone dystrophy associated with supernormal rod response [CDSRR; MIM# 610356; Wu et al., 2006]. This apparently rare form of cone dystrophy is characterized by a congenital or early childhood onset, with poor best-corrected visual acuity (VA), central scotoma, marked photophobia, severe dyschromatopsia, and occasionally nystagmus. Some patients complain of night blindness from childhood onwards or develop night blindness in the later stages of the disease. Fundus findings are highly variable, varying from minute discrete accentuation of the foveal reflexes to unspecific granular changes in the macula; few patients develop foveal or macular retinal pigment epithelium (RPE) atrophy [Michaelides et al., 2005; Wissinger et al., 2008]. A hallmark of CDSRR is the decreased

Additional Supporting Information may be found in the online version of this article.

†Present address: Department for Opthalmology, University Regensburg, Regensburg, Germany.

*Correspondence to: Bernd Wissinger, Molecular Genetics Laboratory, Centre for Ophthalmology, Röntgenweg 11, D-72076 Tübingen, Germany. E-mail: wissinger@uni-tuebingen.de

Contract grant sponsors: Deutsche Forschungsgemeinschaft (KFO 134–KO2176/1-2 (to S.K.), KFO 123–BO2089/1-2 (to M.B.), and LO457/3,1-3 (to B.L.)); Bundesministerium für Bildung und Forschung (HOPE-01GM0850 (to B.W.)); the Foundation Fighting Blindness (to J.H.); The Hungarian National Research Fund (OTKA K75239 (to P.E.)).

and delayed dark-adapted response to dim flashes in electroretinographic (ERG) recordings, which contrasts with the supernormal b-wave response at the highest levels of stimulation. In addition, light-adapted responses to a bright flash and to 30-Hz flickers are delayed and markedly decreased [Gouras et al., 1983; Michaelides et al., 2005]. Several studies have shown that this autosomal recessive inherited phenotype is rather exclusively linked to mutations in *KCNV2* [Ben-Salah et al., 2008; Robson et al., 2010; Sergouniotis et al., 2011; Thiagalingam et al., 2007; Wissinger et al., 2008], and thus strikingly different from the genetic heterogeneity observed for the majority of inherited retinopathies. Up to now 30 different mutations in KCNV2 have been reported. These are almost exclusively small insertion or deletion mutations (so-called indels) and missense or nonsense inducing point mutations. *KCNV2* is predominantly expressed in retinal photoreceptors, most likely in both rods and cones [Czirják et al., 2007; Wu et al., 2006]. It encodes a member of the family of voltage-gated potassium channels (K_v channels), representing a silent subunit (Kv8.2, according to the IUPHAR nomenclature), that does not form functional channels on its own. It has been shown that Kv8.2 is able to assemble with Kv2.1 to form functional heteromeric channels with properties distinct from Kv2.1 homomeric channels, including a shift in the steady-state activation curve toward more negative potentials, a lower threshold potential for activation, a shortened activation time, and slower inactivation kinetics [Czirják et al., 2007]. Heteromeric Kv2.1/Kv8.2 channels show characteristics that resemble the I_{kx} current first observed in amphibian photoreceptors [Beech and Barnes, 1989]. A lack of Kv8.2, as a consequence of a mutation in *KCNV2*, may affect important characteristics of the I_{kx} current, for instance a sustained outward potassium current in the dark, that may influence the photoreceptor membrane potential. However, the mechanisms of dysfunction that link *KCNV2* mutations with the clinical picture of CDSRR still remain to be elucidated.

Subjects, Material and Methods

Patients and family members were recruited over a period of more than 15 years at different clinical centers and venous blood samples were collected after informed consent was obtained.

Ophthalmological Examination

Clinical diagnoses were based on standard ophthalmological examination including evaluation of ocular motility, VA, refraction, color vision and visual field testing, anterior segment pathology using slit lamp examination, fundus examination followed by fundus photography, autofluorescence imaging, and ERG recordings under scotopic and photopic conditions.

Molecular Genetic Analyses

Total genomic DNA was isolated from peripheral blood samples according to standard procedures. Mutation screening of the *KCNV2* gene (cDNA reference sequence NM_133497.3) was carried out by complete sequencing of the coding exons and flanking intronic/untranslated region (UTR) sequences as described previously [Wissinger et al., 2008]. Small heterozygous indel mutations that result in overlaid sequence traces were further confirmed by cloning of PCR products and subsequent sequencing of plasmids from single bacterial colonies.

Deletion breakpoints were bridged by long-distance PCR (LD-PCR) amplifications followed by restriction mapping refinement and finally covered by DNA sequencing applying primer-walking strategy.

Copy number analysis for exon 1 of the *KCNV2* gene was done by quantitative PCR (qPCR) employing TaqMan technology with a custom designed assay as described previously [Wissinger et al., 2008]. Further copy number qPCRs for loci flanking *KCNV2* were performed as follows using SYBR Green for product detection: 20-µl reactions containing 100 ng of genomic DNA, 500 nM of forward and reverse primer, and 10-µl SYBR Green Master Mix (Roche Applied Science, Basel, Switzerland) were subjected to thermal cycling with 5 min at 95°C, followed by 45 cycles of 10 sec at 95°C, 15 sec at 59°C and 30 sec at 72°C on a Lightcycler 480 (Roche Applied Science). An assay that amplifies a fragment at *GAPDH* was used as reference. qPCRs were done in triplicate and mean Ct values were used for calculations. The mean of the ΔCt values ($Ct^{\text{"Target"}} - Ct^{GAPDH}$) of two to four control samples were used as calibrator, and ΔΔCt and $2^{-\Delta\Delta Ct}$ values were calculated for the patient samples to be assessed.

Comparative genome hybridizations (CGH) using a ready-made chromosome 9 specific 385k oligonucleotide array (HG18 CHR9 FT; Roche NimbleGen Inc., Madison, WI) were carried out for two individuals with larger heterozygous deletions at the *KCNV2* locus. Prior to CGH, DNA samples were further purified by phenol/chloroform extraction and checked for DNA integrity by agarose gel electrophoresis. CGH was carried out as a commercial service at Roche NimbleGen, Reykjavik, Iceland.

In order to assess homozygosity regions and potential segments of identity-by-descent, we used restriction-enzyme digested genomic DNA for hybridizations on Affymetrix 250k_NspI single nucleotide polymorphism (SNP) arrays (Affymetrix, Santa Clara, CA). Samples were processed in accordance with the manufacturer's instructions and arrays were scanned with the Affymetrix GeneChip Scanner 3000 7G. Genotypes were called with Affymetrix Genotyping Console Software v2.1 (GTC) using the BRLMM algorithm with default calling threshold of 0.5 and a prior size of 10,000 bases. Samples were required to have a minimum Quality Control SNP call rate of 90%.

Yeast Two-Hybrid Interaction Assays

Yeast two-hybrid bait and prey constructs encoding N-terminal fragments of KCNB1/Kv2.1 (amino acid residues 1–190) and KCNV2/Kv8.2 (amino acid residues 1–257), and cloned into pGBKT7 (as fusion with the Gal4 DNA binding domain) and pGADT7 (as fusion with the Gal4 activation domain) were reported by Ottschytsch et al. [2002] and were kindly provided by Dr. Elke Bocksteins and Dr. Dirk Snyders (Laboratory of Molecular Biophysics, Physiology, and Pharmacology, University of Antwerp, Belgium). Missense mutations were introduced by in vitro mutagenesis using the overlap extension strategy [Ho et al., 1989] and confirmed by DNA sequencing. Purified plasmid DNA was used to transform yeast strains Y2HGold and Y187 (Clontech/Takara Bio Europe, Saint-Germain-en-Laye, France), applying standard protocols. Mated dipoid cells or co-transformed haploid cells were streaked on double dropout (SD-Leu-Trp) and quadruple dropout (SD-Leu-Trp-His-Ade) medium with or without aureobasidin A (125 ng/µl) and X-α-Gal (40 µg/ml), and grown for 72–120 hr at 30°C. β-Galactosidase activity resulting from yeast two-hybrid dependent activation of the LacZ gene expression was determined in lysates of co-transformed Y187 yeast cells using chlorophenyl red b-galactopyranoside (CPRG; Sigma-Aldrich, Taufkirchen, Germany) as substrate according to standard protocols. Mean values and standard deviations of β-Galactosidase activity were calculated from two

replicates of each of three independent yeast colonies using the formula: $1{,}000 \times OD_{570}/(t \times V \times OD_{600})$ with t being the incubation time, V being the dilution factor, and OD_{600} being the cell culture density before harvesting of the cells.

Results

Screening of the *KCNV2* Gene in Patients with an Initial Diagnosis of Cone Dysfunction

Prior studies have shown that the phenotype of CDSRR is exclusively linked to mutations in *KCNV2*. CDSRR was first described in 1983 as a new disease entity [Gouras et al., 1983] and subsequently only few case reports and small patient series have been reported, suggesting that CDSRR is a very rare condition. In order to test whether CDSRR is underdiagnosed or whether *KCNV2* mutations might also be involved in other retinal phenotypes, we applied DNA sequencing to screen for mutations in this gene in a large cohort of 367 independent patients initially referred to us with various diagnoses of cone-related retinal dystrophies including achromatopsia and blue cone monochromacy (n = 167), cone dystrophy (n = 154), and cone-rod dystrophy (n = 43). Patients diagnosed with achromatopsia or blue cone monochromacy were preselected for the absence of mutations in at least *CNGA3* and *CNGB3* [Kohl et al., 1998, 2000; Wissinger et al. 2001], and the cone opsin gene cluster on Xq28, respectively. In addition, we also included three families with CDSRR that were newly diagnosed since our last study. The composition of the patient cohort is listed in Supp. Table S1.

In all three new CDSRR cases, we found *KCNV2* mutations: a homozygous c.1381G>A/p.Gly461Arg mutation in family ZD389 (two affected siblings), compound heterozygous mutations, c.727C>T/p.Arg243Trp and c.794_795dupCC/p.Ser266ProfsX57, in patient RCD425, and compound heterozygous mutations, c.8_11del4/p.Lys3ArgfsX95 and c.775_795dup21/p.Ala259_Ala265dup7, in the index patient of family RCD382 (see Supp. Table S2 for the genotypes of all patients and Table 1 for a list of all mutations and variants identified in this study). This further emphasizes the specificity of the association between CDSRR and *KCNV2* mutation.

In RCD382 (see Fig. 1A for the pedigree), the three sisters of the father had a history of reduced vision with glare, nystagmus, night vision problems since childhood and with maculopathy on external ophthalmological examinations. One affected sister was investigated clinically in detail in comparison with the index patient (Supp. Table S3). At an age of 33 years she demonstrated fine horizontal nystagmus, her VA was 0.03 in both eyes and isopters in Goldmann visual field were constricted for V/4e and III/4e (no smaller/dimmer targets detected). Optic discs appeared normal but her macula had no physiological reflexes. ERGs had signs now known to be typical for mutations in *KCNV2* as summarized in Supp. Table S3 [Friedburg et al., 2007]. The differential diagnosis at the time of investigation was achromatopsia or cone (rod) dystrophy. We found that she and her affected sisters carry the c.775_795dup21 mutation, and in addition a novel heterozygous missense mutation c.989T>C/p.Phe330Ser. The later affects an evolutionary highly conserved phenylalanine residue and was excluded in 75 healthy controls, further supporting that three pathogenic *KCNV2* mutations segregate in this family (Fig. 1A).

Upon screening the sample of patients with an initial diagnosis of other cone-related retinal dystrophies, we found single homozygous or two heterozygous *KCNV2* mutations in a subset of patients: in seven patients with an initial diagnosis of achromatopsia, four patients with cone dystrophy, and one patient with cone-rod dystrophy. Mutations in these patients included two frameshift mutations, two nonsense mutations, one in-frame 9-bp deletion, five missense mutations, and several larger deletions, as described below (Table 1 and Supp. Table S2). None of the point mutations or small indel mutations were observed in healthy controls (n = 59–97). In addition, we found 11 patients (four with a diagnosis of achromatopsia, five with cone dystrophy, and two with cone-rod dystrophy) with single heterozygous mutations. Except for a 9-bp in-frame duplication (c.1133_1141dup/p.Arg386_Ile387dvp), all other single heterozygous mutations represent missense substitutions that have not been observed in other CDSRR patients or controls.

Considering only patients with homozygous or compound heterozygous *KCNV2* mutations, our results indicate that mutations in *KCNV2* account for about 2.2–4.3% of patients with various initial diagnoses of cone dysfunction. Hence, we retrospectively reassessed whether those cases differ from the phenotype of CDSRR. We specifically asked the ophthalmologists in charge, whether—based on the genetic findings—a diagnosis of CDSRR would be more appropriate or specific than the initial diagnosis. Based on follow-up examinations or reevaluation of available clinical data that was done for 10 patients, the answer was positive for nine of these patients (Supp. Table S2). There were different reasons why the patients were initially diagnosed with other retinal dystrophies, for example (1) unawareness of CDSRR, (2) typical features overlooked or not adequately considered, (3) ERG response considered as an artifact, and (4) low-quality ERG data. Only one patient diagnosed with cone dystrophy, who carried two missense mutations (c.491T>C/p.F164S and c.1381G>A/p.G461R), did not fully qualify for a diagnosis of CDSRR, since the bright flash responses in ERG recordings were still in the normal range.

Identification and Characterization of Homozygous Deletions in the *KCNV2* Gene

We repeatedly failed to amplify *KCNV2* exon 1 in two patients (from pedigrees CHRO417 and RCD307 in Fig. 1B), though exon 2 and other genomic loci could be readily amplified. We therefore reasoned that homozygous deletions might be present in those patients. In fact, qPCR-based copy number analysis of *KCNV2* exon 1 in the mother in RCD307 revealed a $2^{-\Delta\Delta Ct}$ value of 0.48, that is, an about 50% reduced copy number. We further pursued with sequence tag site (STS) content mapping and LD-PCR experiments that eventually led to the identification of a deletion of 10,909 bp that encompasses all but the first 18 bp of the coding sequence of exon 1 and most parts of intron 2, and a short 6-bp sequence insertion between the proximal and distal breakpoint (c.19_1356+9571delinsCATTTG; Supp. Fig. S1). Both the mother and the unaffected brother in RCD307 were heterozygous carriers for this mutation (Fig. 1B). Exactly the same mutation was also present in the index patient in CHRO417. There was no evidence of close consanguinity in either family. RCD307 originate from Southern Germany and CHRO417 from Hungary and could not specify any relationship upon personal interview. Still, we suspected a common origin of this very specific deletion + insertion mutation. To evaluate this hypothesis, we performed a comparative high-resolution 250k SNP array analysis with DNA from both patients. We found that both showed significant intervals of homozygosity on chromosome 9p24 (including the *KCNV2* locus) of 8.3 Mb (patient CHRO417) and 1.2 Mb (patient RCD307), respectively (Supp. Fig. S2). Yet, the region of shared SNP genotypes

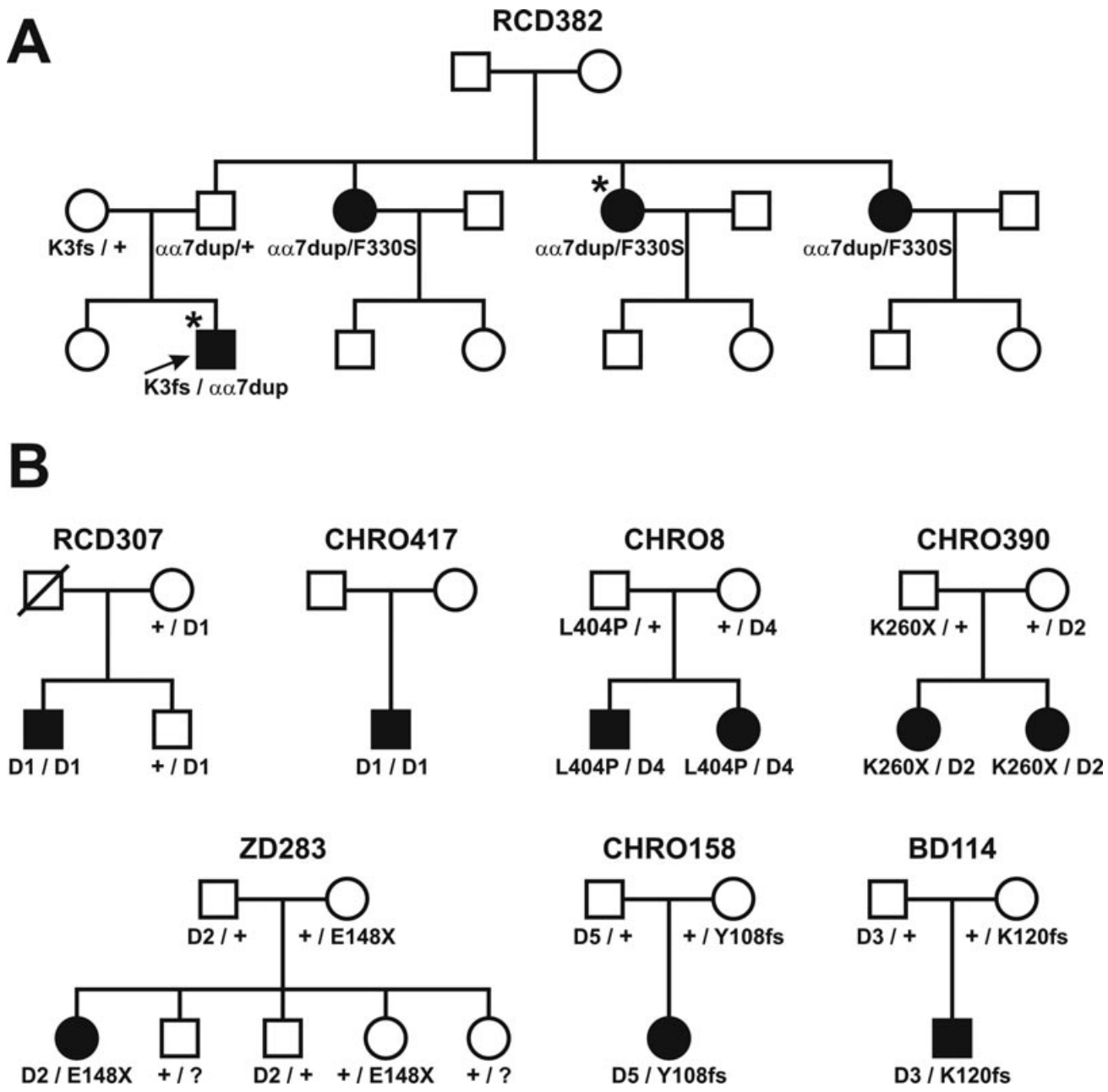

Figure 1. Selected families that segregate *KCNV2* mutations. A: Pedigree of family RCD382, that segregates three *KCNV2* mutations. The arrow marks the index patient and asterisks indicate the patients for which detailed clinical data are provided in Supp. Table S3. B: Pedigrees of the seven families with large deletions at the *KCNV2* locus. Genotypes are given for all probands for which DNA samples were available. Abbreviations of the deletions/mutations are as follows: D1, c.19_1356+9571delinsCATTTG; D2, c.434_*30+154del; D3, g.2696639_2713626del; D4, g.2657638_2737340del; D5, g.2570596_2807413del; αα7dup, c.775_795dup21. "?" in the genotypes for some unaffected members in ZD283 indicates that they have not been tested for the E148X mutation.

between the two patients is rather small with less than 300 kb in size. Nonetheless, a common ancestry of the mutation is very likely, since that interval is covered by 162 SNPs on the high-resolution SNP chip.

Identification and Characterization of Large Heterozygous Deletions at the *KCNV2* Locus

During our initial screening, we found six patients with apparently homozygous point mutations in exon 1 of the *KCNV2* gene, although parental consanguity was not documented in any of these families. Family members for co-segregation analysis were available for five of these six families. Concordant segregation of genotypes was only observed in one family (CHRO246 which segregates the c.1348T>A/p.Trp450Arg mutation), whereas inconsistent segregation was noted in the remaining four families (pedigrees CHRO8, CHRO158, CHRO390, and ZD283, Fig. 1B). In all four families, we observed that the mutation (apparently homozygous in the patient) was only present in heterozygous state in one parent. In order to evaluate the possibility of allelic dropout due to the presence of a heterozygous deletion, we performed qPCR-based copy

Table 1. Mutations and Rare Sequence Variants in the KCNV2 Gene in This Study

Location	Alteration nucleotide sequence[a]	Alteration polypeptide	Total no. of chromosomes[b]	Reference[c]
Mutations				
Exon 1	c.8_11del4	p.Lys3ArgfsX96	3	f
Exon 1	c.323_329del7	p.Tyr108TrpfsX14	1	This article
Exon 1	c.442G>T	p.Glu148X	3	a, b
Exon 1	c.491T>C	p.Phe164Ser	1	This article
Exon 1	c.727C>T	p.Arg243Trp	1	This article
Exon 1	c.778A>T	p.Lys260X	1	a, c
Exon 1	c.782C>A	p.Ala261Asp	2	This article
Exon 1	c.775_795dup21	p.Ala259_Ala265dup7	1	This article
Exon 1	c.794_795dupCC	p.Ser266ProfsX57	1	This article
Exon 1	c.989T>C	p.Phe330Ser	1	This article
Exon 1	c.1016_1024del	p.Asp339_Val341del	1	a, d
Exon 1	c.1211T>C	p.Leu404Pro	1	This article
Exon 1	c.1348T>A	p.Trp450Arg	2	This article
Exon 2	c.1381G>A	p.Gly461Arg	4	a, b, c, f
D1: Exon 1+	c.19_1356+9571 delinsCATTTG	p.Arg7HisfsX57	4	This article
D2: Exon 1+2	c.434_*30+154del	p.Glu145LeufsX4	2	This article
D3: Exon 1+	g.2696639_2713626del	loss	1	a[d]
D4: Complete gene	g.2657638_2737340del	loss	1	This article
D5: Complete gene	g.2570596_2807413del	loss	1	This article
Rare variants				
Exon 1	c.107G>A	p.Arg36His	1	This article
Exon 1	c.190G>A	p.Glu64Lys	1	This article
Exon 1	c.222G>C	p.Glu74Asp	1	This article
Exon 1	c.328C>G	p.Leu110Val	1	This article
Exon 1	c.441C>G	p.Asp147Glu	1	d
Exon 1	c.725A>G	p.Gln242Arg	1	This article
Exon 1	c.853A>T	p.Met285Leu	1	This article
Exon 1	c.874G>A	p.Gly292Ser	1	This article
Exon 1	c.1133_1141dup	p.Leu381_Arg383dup	1	This article
Exon 2	c.1607A>G	p.Asn536Ser	1	This article
Exon 2	c.1616T>C	p.Leu539Pro	1	This article

[a] cDNA Reference Sequence: NM_133497.3 with numbering that denotes the adenosine of the annotated translation start codon as nucleotide position +1. Genomic reference sequence: NT_008413.18.
[b] Chromosomes counted only for the index patients. Homozygous mutations counted as two chromosomes.
[c] References: a, Wissinger et al., 2008; b, Ben-Salah et al., 2008; c, Thiagalingan et al., 2007; d, Wu et al., 2006; e, Robson et al., 2010; f, Sergouniotis et al., 2011.
[d] Described as "gross deletion."

number analysis for *KCNV2* exon 1. This experiment showed a reduced copy number in all tested individuals (affected patients and the transmitting parent) with $2^{-\Delta\Delta Ct}$ values ranging between 0.51 and 0.59 (data not shown), confirming the presence of heterozygous deletions.

For the mapping and characterization of these heterozygous deletions, we performed intrafamilial segregation analysis of polymorphic markers (one STR and 29 SNPs) and qPCR-based copy number analysis (three assays). Based on these approaches, we were able to refine the outermost borders of the deletions in CHRO390, ZD283, and also BD114, a family from our prior study that segregates an as yet uncharacterized heterozygous deletion in *KCNV2* [Wissinger et al., 2008]. Subsequent LD-PCR experiments and primer walking led to the identification of an identical intragenic 11.7-kb deletion (c.434_*30+154del) in both CHRO390 and ZD283, and a 16.9-kb deletion (Chr9:g.2696639_g.2713626del; NCBI Build 36.1 human genome assembly) in BD114 (Supp. Fig. S1 and Fig. 2A). Whereas the first deletion has its junctions within exon 1 and ~150-bp downstream of exon 2, the latter encompasses the complete exon 1 and parts of intron 1.

Deletion mapping by qPCR and segregation analysis in CHRO158 and CHRO8 showed that in both cases the deletions were much larger than in the other families. We therefore performed array CGH experiments employing a chromosome 9 specific 385k NimbleGen oligonucleotide array. In both cases, we observed a clear-cut region of reduced copy number encompassing the *KCNV2* locus (Fig. 2B). We carefully examined the probes at the edges of the deduced deletions in order to design primers for LD-PCR. This approach eventually led to the successful amplification of junction fragments and the subsequent determination of the breakpoint sequences. These experiments revealed a 79.7-kb deletion in CHRO8 (Chr9:g.2657638_g.2737340del) and a 237-kb deletion (Chr9:g.2570596_g.2807413del) in CHRO158 (Fig. 2 and Supp. Fig. S1). In both instances the *KCNV2* gene is completely deleted. In CHRO158 the deletion additionally encompasses the entire *VLDLR* gene, and eliminates the first exon of *LOC401491/FLJ35024*, a transcript cluster annotated as a long noncoding RNA, as well as the five terminal coding exons of *KIAA0020*, a putative protein coding gene of unknown function.

Analysis of Deletion Junctions and Putative Deletion Mechanisms

Analysis of the deletion junctions revealed microhomology of 2 to 6 bp in length and in one case an insertion of 6 bp (Supp. Fig. S1). Five of the 10 breakpoints are located in diverse repetitive DNA sequence elements (LINE, SINE, transposon-derived). When compared with BLAST 2-Sequences, none of the breakpoint junction sequence pairs (±500 bp relative to each breakpoint) showed segments of sequence homology that may be indicative for a homology-based mechanism underlying the deletion. We therefore propose nonhomologous end joining (NHEJ), a mechanism that rather accurately rejoins double-strand breaks (DSBs), as the most likely mechanism. Notably, we have not observed recurrent independent deletions and

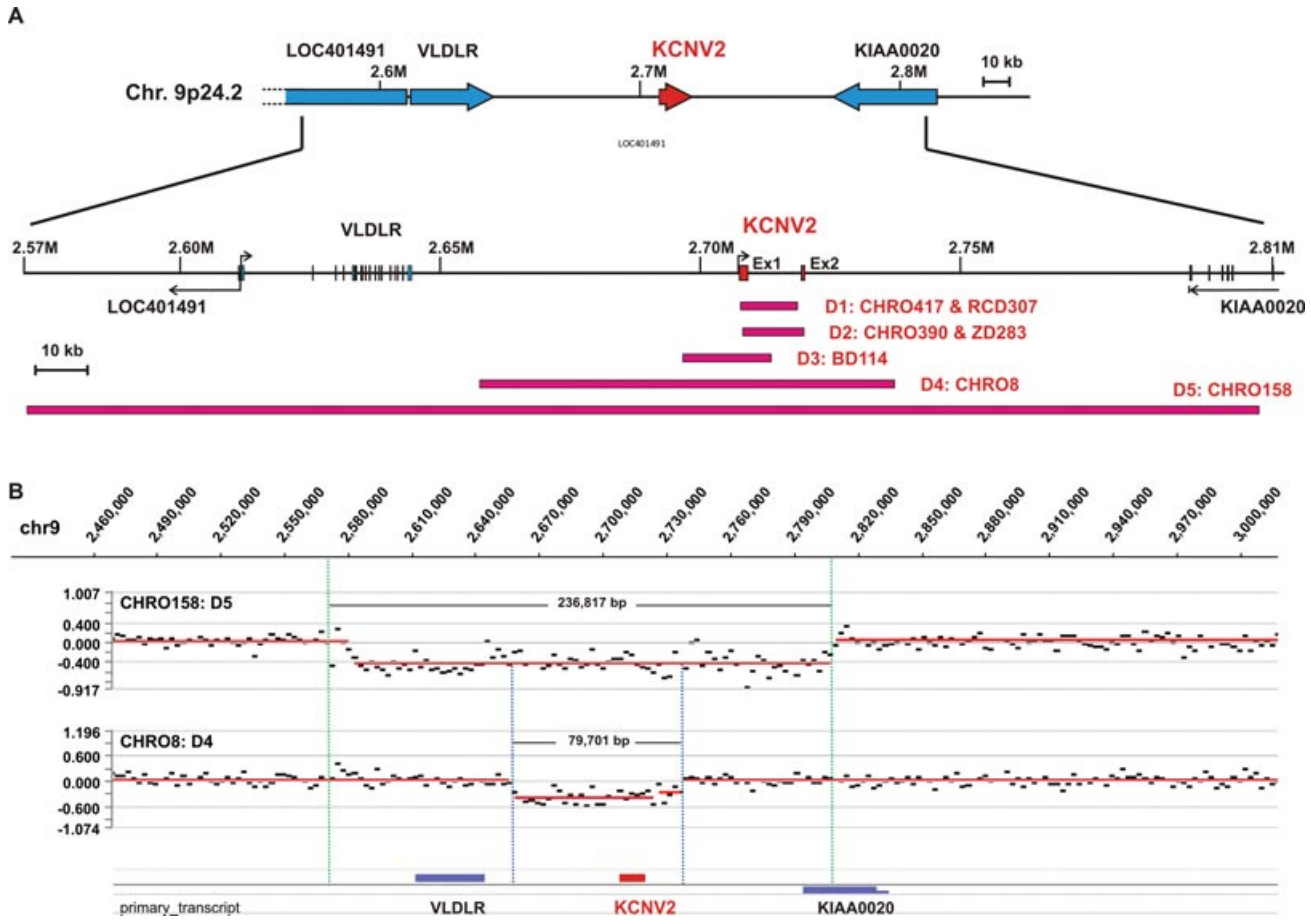

Figure 2. Mapping of deletions at the *KCNV2* locus. A: Overview of the size and coverage of the deletions at the *KCNV2* locus in this study. B: Deletion detection by array-based CGH. Shown are the results of the CGH performed with a 385k chromosome 9 specific Nimblegen oligonucleotide array. The analyzed affected family members of families CHRO8 (top) and CHRO158 (bottom) displayed clear region of reduced copy number (averaged probe intensities) at the *KCNV2* locus.

the deletions breakpoints are rather dispersed except for deletions D1 and D3 in which breakpoints are 415 bp (telomeric side) and 1245 bp (centromeric side) apart. Moreover, there are only few copy number variants (CNVs) from genome-wide studies that map to this region on chromosome 9 (as listed in the UC Santa Cruz Genome browser). These include four copy number losses (size range: 603–20,657 bp) and three copy number gains (size range: 580–1185 bp), all of them localize either upstream or downstream of *KCNV2*.

As a whole, the 237 kb region that encompasses all deletions has a GC content of 40.4% and is enriched for repetitive sequences. A total of 47.2% of the region does represent repetitive sequences compared with an average of 43% for human genome sequences with similar GC content [Smit 1999]. This difference is mainly due to a disproportionately high number of MIR and LTR elements: 4.3% versus 2.3% and 14.4% versus 8.6%, respectively. Yet, the increase in repetitive sequences in the deletion region is not uniform, but mostly restricted to the centromeric half, where its content is as high as 56.8%. The meiotic recombination rate in that region is rather high, on average 2.53 cM/Mb. The region contains four strong recombinational hotspots with a recombination rate >20 cM/Mb (Supp. Fig. S3; hotspots 1–3 and 6) and three weak hotspots with a recombination rate >5 cM/Mb (Supp. Fig. S3; hotspots 4, 5, and 7). Notably three of the five telomeric deletion breakpoints localize to these hotspots including D4-tel that maps to the strong hotspot #2 and one centromeric breakpoint localizes in the close vicinity of a weak hotspot (Supp. Fig. S3). Since NHJE involves rejoining of DSBs one might argue that either the deletions may have occurred during meiotic recombination or that recombinational hotspots per se favor the occurrence of DSBs.

Missense Mutations in the NAB Domain Affect Assembly with Kv2.1

Besides protein truncation mutations and larger deletions described in this article, missense mutations do represent a substantial fraction of all *KCNV2* mutations reported so far with clusters in the pore domain and the N-terminal segment of the protein [Ben-Salah et al., 2008; Thiagalingam et al., 2007; Wissinger et al., 2008; Wu et al., 2006]. The N-terminal segment of voltage-gated potassium (Kv) channels contains conserved sequence motifs (called NAB: N-terminal A and B box domain or T1: N-terminal tetramerization domain, Supp. Fig. S4), which are required for homomeric as well as heteromeric channel recognition and assembly. Kv8.2 (the gene product *of KCNV2*) represents a modulatory channel subunit that is able to form heteroligomeric channels with Kv2.1 in vitro [Czirjak et al., 2007; Ottschytsch et al., 2002]. We therefore wondered whether mutations in the NAB domain of Kv8.2 might affect assembly with Kv2.1 (Supp. Fig. S4). To address this question, we applied yeast two-hybrid technology using the Kv8.2 ($\alpha\alpha$1-250) as prey and Kv2.1 ($\alpha\alpha$1-190) as bait. Wild-type Kv8.2 showed strong

A

	Kv2.1	Kv8.2 -WT	Kv8.2 -L110V	Kv8.2 -D147E	Kv8.2 -F164S	Kv8.2 -E184K	Kv8.2 -E184V	Vector
Kv2.1	+++	++++	+	++	+	-	-	-

B

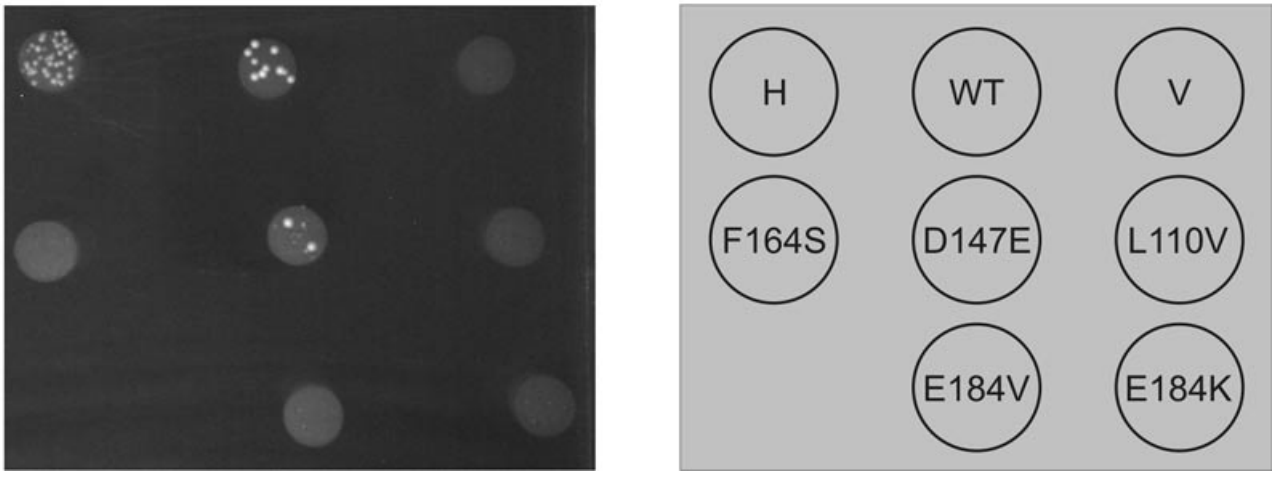

Figure 3. Yeast two-Hybrid phenotype of N-terminal amino acid substitution mutants in KCNV2. Yeast two-hybrid interaction assays were performed using N-terminal fragments of Kv2.1 and Kv8.2 (gene product of *KCNV2*) as bait and prey, respectively. **A:** Qualitative assessment of growth and α-Gal blue coloring of co-transformed yeast colonies on double and quadruple dropout medium with or without aureobasidin. **B:** Growth of co-transformed yeasts on quadruple dropout medium including aureobasidin after 5 days at 30°C. H, homomeric interaction with Kv2.1 as both bait and prey; WT, wild-type Kv8.2; V, co-transformation with empty bait vector.

interaction with Kv2.1 in this assay (as assessed by colony number and size on quadruple dropout medium, and the timing and intensity of α-Galactosidase-based blue staining of colonies). In contrast, we observed that the F164S mutant Kv8.2 fragment (representing a novel mutation described in this article) exhibit reduced interaction, and that E184K as well as E184V mutant Kv8.2 fragments [representing two previously reported *KCNV2* mutations; Wissinger et al. 2008] showed no evidence of interaction with the Kv2.1 fragment (Fig. 3). We also used this assay to analyze the functionality of two other nonsynonymous sequence variants, L110V and D147E, which were found as single heterozygous variants in individual patients. We noted that the D147E variant yielded a growth and color phenotype that outperformed any of the Kv8.2 mutants, whereas the L110V variant exhibit a phenotype of reduced growth comparable with that of the F164S mutant. To quantify these results, we performed interaction-based β-galactosidase activity measurements in lysates of yeasts co-expressing Kv2.1 and wild-type or mutant Kv8.2 fragments, respectively. This assay showed a virtual absence of activity (not significantly different from the negative control) for the E184K and the E184V mutant, respectively, and an about 70-fold reduced activity of both the F164S and the L110V variants compared with the wild-type Kv8.2 protein fragment (Fig. 4). In contrast, we found that the D147E variant exhibited an activity that is still about one-third of the activity of the wild-type.

From these data we conclude that missense mutations that affect the N-terminal portion of Kv8.2 interfere with the interaction between Kv8.2 and Kv2.1, and probably preclude proper assembly of heterooligomeric channels in vivo.

Discussion

Several studies have shown that the phenotype of CDSRR is virtually always associated with mutations in *KCNV2* [Ben-Saleh et al., 2008; Robson et al., 2010; Thiagalingan et al., 2007; Wissinger et al., 2008; Wu et al., 2006]. However, it has not yet been investigated whether mutations in *KCNV2* might also cause other forms of retinopathies, as is the case with several other retinal disease genes (for instance mutations in *ABCA4*, *RDS*, or *NR2E3*). Upon screening of a large cohort of patients with an initial diagnosis of achromatopsia, cone dystrophy, and cone-rod dystrophy, we found a fraction of 2.2–4.3% of patients who carried either homozygous or compound heterozygous mutations in *KCNV2*. Retrospective analysis of the clinical data or clinical reinvestigation of the available patients revealed that their phenotype was indeed fully compatible with a diagnosis of CDSRR, except for one patient in which the bright flash ERG responses were still in the normal range. It has been reported that there is variability in the ERG responses in CDSRR patients and the amplitude of the rod b-wave might not be an unambiguous criterion for CDSRR. Other features such as elevated b-/a-wave ratios in the mixed rod-cone response and the marked prolongation of b-wave implicit times with a steep amplitude versus intensity relationship might be even more helpful in the differential diagnosis [Friedburg et al., 2007; Nagy et al., 2009].

Our study showed that CDSRR is not as rare as previously thought. Therefore, CDSRR should be kept in mind in patients with early onset, slowly progressive cone dystrophy and a thorough electrophysiological examination is warranted, with an ERG which

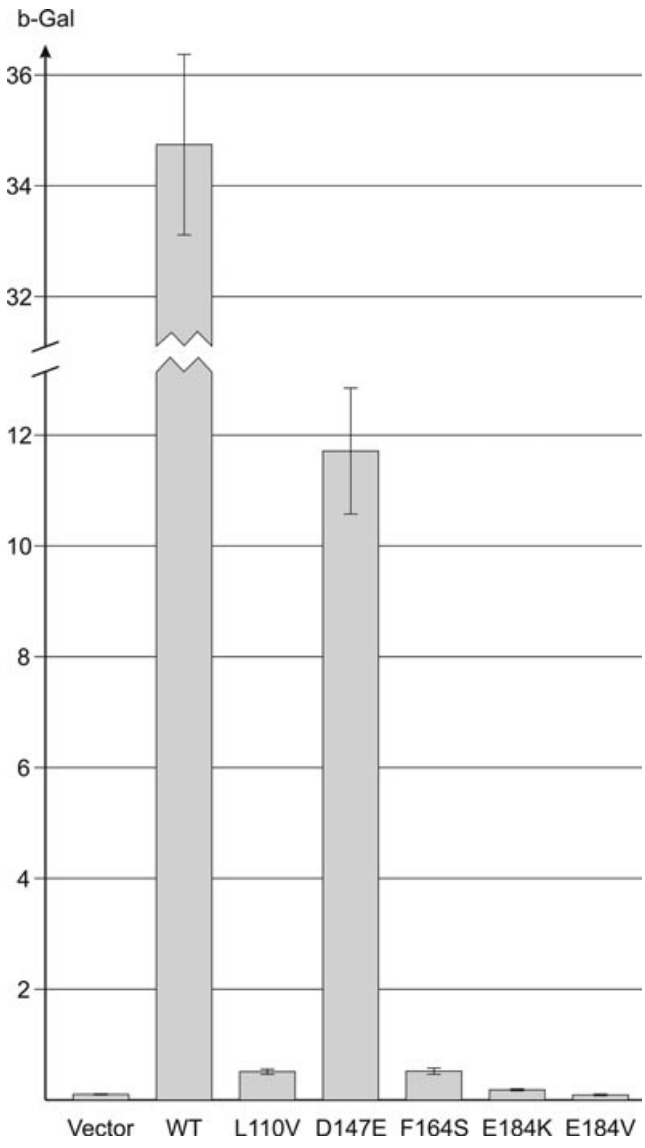

Figure 4. Yeast two-Hybrid based β-Galactosidase activity of KCNV2 wild-type and mutants. Co-transformed Y187 yeast cells were lysed and the β-Galactosidase activity determined by a colorimetric assay using CPRG as substrate. Mean values and standard deviations of the activity were calculated from duplicate measurements of three independent colonies per co-transformation. Note that the Y-axis is interrupted to display the high activity of the wild-type construct.

preferentially is not limited to the standard protocol recommended by the International Society of Clinical Electrophysiology, but also includes an intensity series in the dark-adapted patient.

A main outcome of our study is the identification and characterization of larger deletions encompassing *KCNV2*. Except for a homozygous deletion covering exon 2 [Robson et al., 2010] and an uncharacterized "gross deletion" reported in our previous article [Wissinger et al., 2008], no other larger deletions have as yet been reported for *KCNV2*. Our data show that such deletions do represent a substantial fraction of all mutant *KCNV2* alleles. If we compile the data of this and our previous study, we end up with a prevalance of 15.5% (9/58) of large deletions among all *KCNV2* mutant alleles. The identification of large deletions was largely due to the genotyping of the parents of patients with apparently homozygous mutations. All five different deletions were much larger than the usual amplicon size in PCR-based mutation screenings and would have been missed without segregation analysis. We therefore strongly recommend that parental segregation analysis should be performed in patients with apparently homozygous *KCNV2* point mutations. Alternatively, CNV analysis either by qPCR, multiplex ligation-dependent probe amplification (MLPA), or CGH should be done when samples of the parents are not available.

Two of the large deletions encompass the entire *KCNV2* gene and the remaining alleles are lacking large parts of the gene. We therefore reason that all these deletions represent null alleles for *KCNV2*. Ranging from 10.9 to 236.8 kb, the sizes of the deletions differ considerably. Except for deletion D5, none of the others affect additional genes besides *KCNV2*. D5 additionally encompasses the entire *VLDLR* gene, and parts of two hypothetical genes (LOC401491/*FLJ35024* and *KIAA0020*). Mutations in *VLDLR* have been recently described in autosomal recessive inherited cerebellar hypoplasia and mental retardation [Boycott et al., 2005], which is also associated with quadrupedal locomotion in some pedigrees [Ozcelik et al., 2008; Türkmen et al., 2008]. In addition and interesting for ophthalmologists, *Vldlr* knock-out mice develop intraretinal neovascularization with choroidal anastomosis and has been studied as models for retinal angiomatous proliferation (RAP), a subtype of exudative age-related macular degeneration [Heckenlively et al, 2003; Li et al., 2007]. Not unexpectedly, there was no evidence for either a neurological or a retinal angiogenic proliferation phenotype in the affected patient in family CHRO158, since he is heterozygous for the D5 deletion and carries a small 7-bp deletion in *KCNV2* (c.323_329del7) on the other allele. However, due to the inclusion of both *KCNV2* and *VLDLR* within the deletion, this single mutation gives rise to carriership status for multiple diseases.

We determined the telomeric as well as the centromeric breakpoints of all five different deletions. Two of the deletions (D1 and D5) are accompanied by small insertions (6 bp and 2 bp, respectively) of extra nucleotides at the site of deletion, whereas the remaining three were precise deletions without any additional sequence rearrangement. There were only very short stretches of 2 to 6 bp conserved between telomeric and centromeric junctions of each deletion, which rules out a homology-based mechanism but rather suggests nonhomologous end joining of DSBs as the most likely origin of the deletions.

Besides large deletions and nonsense mutations, a considerable fraction of potentially pathogenic missense mutations in *KCNV2* have been described. Although as a general practice for a recessive condition, the attribute "mutation" is commonly accepted in cases of homozygosity or in compound heterozygous state with another known mutation and its exclusion in a substantial number of controls, the additional validation by functional assays provide a much higher level of confidence. This holds true in particular for so-called private mutations, which have been found in single families or individuals only. In this study and in our previous investigation we have identified several such private missense mutations, three of them affecting amino acid residues at the N-terminus of KCNV2 (p.Phe164Ser, p.Glu184Lys, and p.Glu184Val). All three localize to the NAB domain of the protein that is required for recognition and assembly of homo- and heterotetrameric Kv channels [Wu et al., 1996; Xu et al., 1995; Supp. Fig. S4]. Previous studies have shown that Kv8.2, the gene product of *KCNV2*, assemble with Kv2.1 to form heterooligomeric channels with distinct biophysical properties [Czirjak et al., 2007; Ottschytsch et al., 2002]. Using yeast two-hybrid technology we comparatively assayed the interaction of the NAB domain of Kv2.1 with wild-type and mutant N-terminal fragments of Kv8.2. Our data convincingly demonstrate either a

drastically reduced or even complete lack of interaction of all three tested mutants compared with the wild-type fragment and thus provide further support and evidence for the pathogenicity of these mutations. The sensitivity of the assay prompted us to analyze two further variants p.Leu110Val and p.Asp147Glu, unclassified rare sequence variant observed as single heterozygous substitutions. The strongly reduced interaction that was observed for the p.Leu110Val variant, suggests that this variant most likely represents a pathogenic mutation, although it may not account for the retinal disease in the patient carrying this mutation, since he is lacking a second mutation.

Based on the autosomal recessive inheritance and the large number of presumptive null alleles (e.g., complete gene deletions, early stop or frameshift mutations), one might reason that CDSRR results from the (functional) absence of the gene product. In line with this argumentation, we suggest that Kv8.2 mutants with amino acid substitutions in the NAB domain (as caused by missense mutations) fail to assemble with Kv2.1 that represents the most likely native counterpart. This might either prohibit the formation of any functional Kv channel or result in pure homomeric Kv2.1 channels that lack the functional tuning of the Kv8.2 subunit for proper native function in photoreceptors.

Acknowledgments

We would like to thank the patients and family members for participating in this study. We also thank Elke Bocksteins and Dirk Snyders (Laboratory of Molecular Biophysics, Physiology, and Pharmacology, University of Antwerp, Belgium) for the yeast bait and prey constructs.

References

Beech DJ, Barnes S. 1989. Characterization of a voltage-gated K+ channel that accelerates the rod response to dim light. Neuron 3:573–581.

Ben-Salah S, Kamei S, Sénéchal A, Lopez S, Bazalgette C, Bazalgette C, Eliaou CM, Zanlonghi X, Hamel CP. 2008. Novel KCNV2 mutations in cone dystrophy with supernormal rod electroretinogram. Am J Ophthalmol 145:1099–1106.

Boycott KM, Flavelle S, Bureau A, Glass HC, Fujiwara TM, Wirrell E, Davey K, Chudley AE, Scott JN, McLeod DR, Parboosingh JS. 2005. Homozygous deletion of the very low density lipoprotein receptor gene causes autosomal recessive cerebellar hypoplasia with cerebral gyral simplification. Am J Hum Genet 77:477–483.

Czirják G, Tóth ZE, Enyedi P. 2007. Characterization of the heteromeric potassium channel formed by kv2.1 and the retinal subunit kv8.2 in *Xenopus oocytes*. J Neurophysiol 98:1213–1222.

Friedburg C, Schambeck M, Bonin M, Kohl S, Wissinger B, Lorenz B. 2007. Ocular phenotype in 3 young siblings with a homozygous KCNV2 mutation followed for 14 years. Invest Ophthalmol Vis Sci 48:E3683.

Gouras P, Eggers HM, MacKay CJ. 1983. Cone dystrophy, nyctalopia, and supernormal rod responses. A new retinal degeneration. Arch Ophthalmol 101:718–724.

Heckenlively JR, Hawes NL, Friedlander M, Nusinowitz S, Hurd R, Davisson M, Chang B. 2003. Mouse model of subretinal neovascularization with choroidal anastomosis. Retina 23:518–522.

Ho SN, Hunt HD, Horton RM, Pullen JK, Pease LR. 1989. Site-directed mutagenesis by overlap extension using the polymerase chain reaction. Gene 77:51–59.

Kohl S, Baumann B, Broghammer M, Jägle H, Sieving P, Kellner U, Spegal R, Anastasi M, Zrenner E, Sharpe LT, Wissinger B. 2000. Mutations in the CNGB3 gene encoding the β-subunit of the cone photoreceptor cGMP-gated channel are responsible for Achromatopsia (ACHM3) linked to chromosome 8q21. Hum Mol Genet 9:2107–2116.

Kohl S, Marx T, Giddings I, Jägle H, Jacobson SG, Apfelstedt-Sylla E, Zrenner E, Sharpe LT, Wissinger B. 1998. Total colorblindness is caused by mutations in the gene encoding the α-subunit of the cone photoreceptor cGMP-gated cation channel. Nat Genet 19:257–259.

Li C, Huang Z, Kingsley R, Zhou X, Li F, Parke DW, Cao W. 2007. Biochemical alterations in the retinas of very low-density lipoprotein receptor knockout mice: an animal model of retinal angiomatous proliferation. Arch Ophthalmol 125:795–803.

Michaelides M, Holder GE, Webster AR, Hunt DM, Bird AC, Fitzke FW, Mollon JD, Moore AT. 2005. A detailed phenotypic study of "cone dystrophy with supernormal rod ERG". Br J Ophthalmol 89:332–339.

Nagy D, Kohl S, Zrenner E, Wissinger B, Jägle H. 2009. Detailed functional and morphological analysis in patients with cone dystrophy with supernormal rod response due to mutations in the Kcnv2 gene. Invest Ophthalmol Vis Sci 50:E4757.

Ottschytsch N, Raes A, Van Hoorick D, Snyders DJ. 2002. Obligatory heterotetramerization of three previously uncharacterized Kv channel alpha-subunits identified in the human genome. Proc Natl Acad Sci USA 99:7986–7991.

Ozcelik T, Akarsu N, Uz E, Caglayan S, Gulsuner S, Onat OE, Tan M, Tan U. 2008. Mutations in the very low-density lipoprotein receptor VLDLR cause cerebellar hypoplasia and quadrupedal locomotion in humans. Proc Natl Acad Sci USA 105:4232–4236.

Robson AG, Webster AR, Michaelides M, Downes SM, Cowing JA, Hunt DM, Moore AT, Holder GE. 2010. "Cone dystrophy with supernormal rod electroretinogram": a comprehensive genotype/phenotype study including fundus autofluorescence and extensive electrophysiology. Retina 30:51–62.

Sergouniotis PI, Holder GE, Robson AG, Michaelides M, Webster AR, Moore AT. 2011. High-resolution optical coherence tomography imaging in KCNV2 retinopathy. Br J Ophthalmol:May 10. [Epub ahead of print; PMID-No: 21558291]

Smit AF. 1999. Interspersed repeats and other mementos of transposable elements in mammalian genomes. Curr Opin Genet Dev 9:657–663.

Thiagalingam S, McGee TL, Weleber RG, Sandberg MA, Trzupek KM, Berson EL, Dryja TP. 2007. Novel mutations in the KCNV2 gene in patients with cone dystrophy and a supernormal rod electroretinogram. Ophthalmic Genet 28:135–142.

Türkmen S, Hoffmann K, Demirhan O, Aruoba D, Humphrey N, Mundlos S. 2008. Cerebellar hypoplasia, with quadrupedal locomotion, caused by mutations in the very low-density lipoprotein receptor gene. Eur J Hum Genet 16:1070–1074.

Wissinger B, Dangel S, Jägle H, Hansen L, Baumann B, Rudolph G, Wolf C, Bonin M, Koeppen K, Ladewig T, Kohl S, Zrenner E, Rosenberg T. 2008. Cone dystrophy with supernormal rod response is strictly associated with mutations in KCNV2. Invest Ophthalmol Vis Sci 49:751–757.

Wissinger B, Gamer D, Jägle H, Giorda R, Marx T, Mayer S, Tippmann S, Broghammer M, Jurklies B, Rosenberg T, Jacobson SG, Sener EC, Tatlipinar S, Hoyng CB, Castellan C, Bitoun P, Andreasson S, Rudolph G, Kellner U, Lorenz B, Wolff G, Verellen-Dumoulin C, Schwartz M, Cremers FP, Apfelstedt-Sylla E, Zrenner E, Salati R, Sharpe LT, Kohl S. 2001. CNGA3 mutations in hereditary cone photoreceptor disorders. Am J Hum Genet 69:722–737.

Wu H, Cowing JA, Michaelides M, Wilkie SE, Jeffery G, Jenkins SA, Mester V, Bird AC, Robson AG, Holder GE, Moore AT, Hunt DM, Webster AR. 2006. Mutations in the gene KCNV2 encoding a voltage-gated potassium channel subunit cause "cone dystrophy with supernormal rod electroretinogram" in humans. Am J Hum Genet 79:574–579.

Wu W, Xu J, Li M. 1996. NAB domain is essential for the subunit assembly of both α-α and α-β complexes of shaker-like potassium channels. Neuron 16:441–453.

Xu J, Yu W, Jan YN, Jan LY, Li M. 1995. Assembly of voltage-gated potassium channels. J Biol Chem 270:24761–24768.